Characteristics of Elastic Waves Generated by Fatigue Crack Penetration and Growth in an Aluminum Plate

Seok-Hwan Ahn, Ki-Woo Nam*
College of Engineering, Pukyong National University,
100 Yongdang-dong, Nam-gu, Busan 608-739, Korea

The characteristics of elastic waves emanated from crack initiation in 6061 aluminum alloy subjected to fatigue loading are investigated through experiments. The objective of the study is to determine the differences in the properties of the signals generated from fatigue test and also to examine if the sources of the waves could be identified from the temporal and spectral characteristics of the acoustic emission (AE) waveforms. The signals are recorded using non-resonant, flat, broadband transducers attached to the surface of the alloy specimens. The time dependence and power spectra of the signals recorded during the tests were examined and classified according to their special features. Six distinct types of signals were observed. The waveforms and their power spectra were found to be dependent on the crack propagation stage and the type of fracture associated with the signals. The potential application of the approach in health monitoring of structural components using a network of surface mounted broadband sensors is discussed.

Key Words : Leak-Before-Break (LBB), Pressure Vessels, Waveform, Power Spectrum, Nondestructive Technique, Acoustic Emission, Surface Crack Propagation, Crack Penetration, Fatigue

1. Introduction

The leak-before-break (LBB) design philosophy used for pressure vessels and energy-related plants (IMCO, 1975 ; Kawahara, 1975 ; Sakai, 1975 ; Kaufman, 1980 ; Miyoshi, 1988 ; Gilchrist, 1992) has been attracting much attention from the point of view of safety and economy. The LBB design aims to insure that content leakage will be detected before the component is subjected to catastrophic failure caused by unstable crack growth. In this sense, the LBB design can be considered as a fail-safe design. The design, however, requires that failure does not occur before cracks have propagated fully through the thickness, and that even after this event, unstable fracture does not occur for some fixed period of time. Many researchers have performed for various aspects (Kim, 1995 ; Huh, 2000 ; Choi, 2001 ; Nam, 2002). It is difficult to evaluate quantitatively the fatigue crack behavior after the penetration due to the fact that quantitative studies of fatigue crack propagation behavior under low fatigue stresses, in three-dimensional, through-crack models are relatively sparse. Ando et al. (Ando, 1987) have proposed a simplified evaluation model for determining the stress intensity factor after penetration. They found that the crack propagation characteristics, the crack shape change, and the crack opening displacement in a variety of specimens could be evaluated using their model.

Acoustic emission monitoring is a very sensitive method with a wide dynamic range and can be used as diagnostics for continuous assessment

* Corresponding Author,
E-mail : namkw@pknu.ac.kr
TEL : +82-51-620-1640; **FAX** : +82-51-624-0746
College of Engineering, Pukyong National University, 100 Yongdang-dong, Nam-gu, Busan 608-739, Korea.
(Manuscript **Received** June 24, 2002; **Revised** August 12, 2003)

of damage in materials and components. Methods based on acoustic emission can be applied to metallic as well as composite structural components subjected to static as well as fatigue loading (Liptai, 1971). In general, acoustic emission can be used to monitor crack initiation and propagation and to locate the source of the emission. Numerous studies have been conducted to determine the correlation between the characteristics of AE output and various fracture mechanics and fatigue damage parameters. It has been shown that under monotonic loading AE can be used to detect yielding and that the cumulative AE output from a notched specimen is directly related to the stress intensity factor (Dunegan, 1969). Acoustic emission has been very useful in detecting crack initiation and propagation under fatigue loading (Kohn, 1992; Fang, 1993).

In this study, the AE technique is applied to study the signal characteristics emanating from fatigue crack propagation and penetration in 6061 aluminum plates under fatigue loading. The AE waveforms generated during various stages of crack propagation and their power spectra are analyzed and classified. The waveforms generated during different stages of crack propagation are shown to have different specific characteristics that can be used to identify the evolution of fatigue cracks in structures through careful analysis of the waveforms captured by broadband sensors located in the structure.

2. Experiment

The specimens used in the experiments are 6061 aluminum alloys; their geometry and dimensions are shown in Fig. 1. The notches were made on one side of the specimens using electric discharge machine (EDM). In all specimens, the initial notch length, $2a_0$, is 8.8 mm and the crack depth, b_0, is 2.4 mm. To reduce noise, the grip sections of the specimens were covered with epoxy and cured by heat treatment for 20 minutes at 80℃. Clay was wrapped around the top and bottom shaft of the test machine as additional damper.

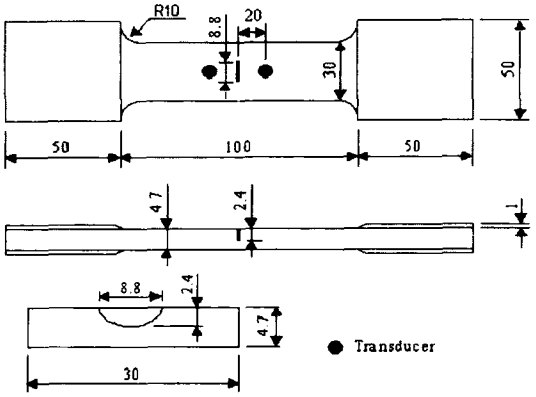

Fig. 1 Geometry of the test specimen. All dimensions are in millimeters

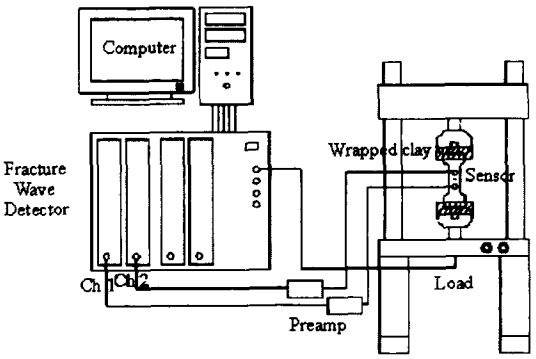

Fig. 2 Measurement system of AE signals

The fatigue tests were performed at room temperature using a servo-hydraulic fatigue testing machine (INSTRON model 8501) under controlled load. The load condition used in the tests was : $P_{max}=15.7$ kN , $R=0.1$. The load cycle was a sine wave of frequency 2 Hz. With both specimens, labeled AT1 and AT2, the test was carried out until fracture after surface crack (initial notch) penetrates the plate thickness. But, the specimen AT2 had retardation period after crack penetration to classify signal characteristics under load reduction.

The measurement systems are shown in Fig. 2. The AE measurements were carried out using a Fracture Wave Detector (FWD) (Model F4000, Digital Wave Corp., Englewood, Co.). The FWD has a digitization resolution of 8 bits, and it allows digitization of the waveforms in real time. The digitization rate was set to 12.5 MHz with a

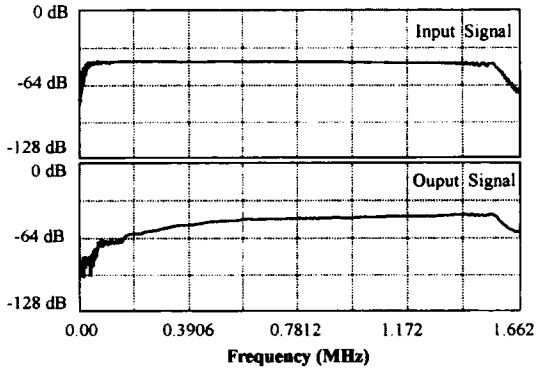

Fig. 3 Swept sine wave face-to-face calibration of B1025 sensors

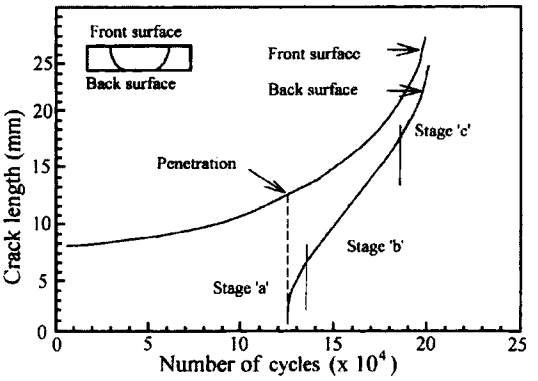

Fig. 4 Schematic diagram of crack propagation behavior in surface crack

1024 point gate length for each channel using a threshold of 0.2 V. Two broadband transducers (DWC B1025), with reasonably flat response to about 1.5 MHz (Fig. 3), were placed at equal distances of 20 mm from the notch (see Fig. 1). Two preamplifiers (AET 140B) with 40 dB gain and 30 kHz-2 MHz plug-in filters were used in the experiments. The gain in the amplifier was set at 20 dB.

3. Fatigue Crack Propagation Behavior

The propagation behavior of the crack initiated at the notch is shown in Fig. 4, based on similar studies carried out earlier in metallic specimens (Nam, 1993, 1994, 1995). The crack length on the initial notch surface (front surface) and the crack length on the penetrated surface (back surface) were measured using a stereomicroscope. The length of the crack on the front surface of the plate grows continuously with no significant effect from the propagation of the crack through the thickness of the plate and its penetration of the back surface.

The propagation characteristics of the crack on the back surface of the plate can be approximately classified into three stages as sketched in Fig. 4. Stage 'pre-penetration' applied to the period before crack penetration through the plate thickness. Stage, "a" applies to the period immediately after crack penetration through the plate thickness;

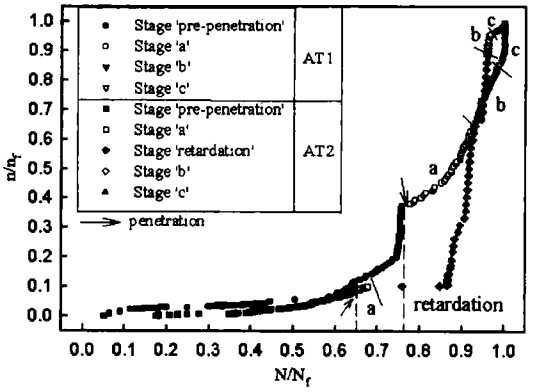

Fig. 5 Relationship between normalized signals and normalized load cycles. Note that there was crack retardation through the back surface in specimen AT2 only

where the trace of the crack grows at a rapid rate. During stage 'b' the trace of the crack grows at an almost constant rate until it reaches a certain length. Finally, in stage 'c', the crack accelerates and the length of the crack trace on the back surface approaches that on the front surface. The AE signals during crack propagation were categorized into five stages: pre-penetration, a, b, c and retardation.

The normalized cumulative signals are plotted versus normalized cycles for the two specimens, AT1 and AT2, in Fig. 5. Here n is the number of signal for a given cycle and n_f is the total number of signals recorded at fracture cycle. N is the number of cycle for a given signal and N_f is the

final number of cycles at fracture. In order to insure that the signals are from the crack or cracks initiated at the notch, only the signals detected at the two sensors at about same time were retained ; the other signals are noise from various sources and were discarded. In both specimens the production of AE signals was initially slow, but it increased rapidly as the crack approached the back surface, and decreased just before penetration. The increase and decrease of the AE signals as the crack approached the back surface can be attributed to the transition of the state of deformation from plane strain to plane stress conditions (Ando, 1985). It can be judged that this is the difference of plastic zone size. That is, even though the crack tip zone is plane strain condition when the crack propagates to bottom direction, plane stress condition with local plastic deformation as the ligament is thinning when the crack approaches to penetrate wall thickness. But, the after-penetration is again plane strain condition as crack propagates to width direction. This tendency was also observed in SS41 steel (Nam, 1999).

In specimen AT1, the number of AE signals increased rapidly with continued cyclic loading after crack penetration. In the stage 'retardation' of specimen AT2, the signals went down significantly just after load reduction. This is due to the fact that at the high load before load reduction, plastic deformation occurred near the crack tip, and the residual plastic stress was relieved by subsequent cyclic loading (Elber, 1970).

4. Signal Characteristics

Since the surface trace of the initial crack (EDM notch) is larger than its depth (Fig. 1), the stress intensity factor at the bottom of the notch is larger than that at the edges of its surface trace. For specimen AT1 the initial stress intensity factor at the front surface is approximately given by, $K_{fs}=9.95\ MPa(m)^{1/2}$, and at the bottom it is, $K_b=11.26\ MPa(m)^{1/2}$. Therefore, the crack initiates first at the bottom of the notch and propagates more rapidly than its front surface trace. The front surface crack initiates and propagates

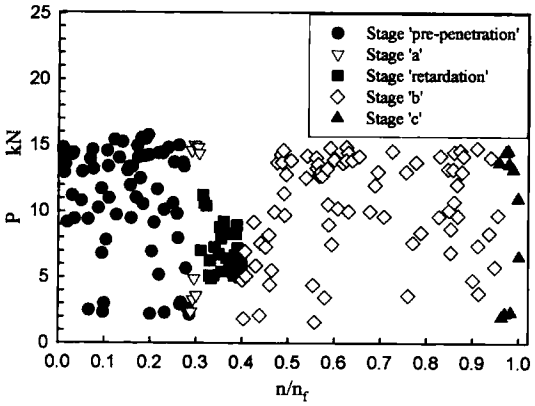

Fig. 6 Relationship between load and normalized signals at different stages of crack growth from specimen AT2

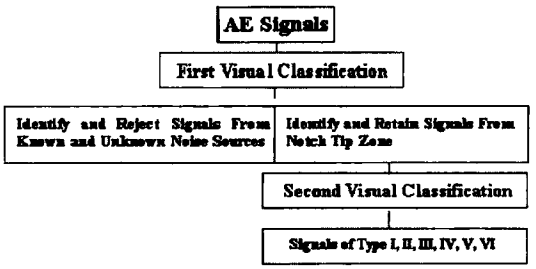

Fig. 7 Flow chart of the visual classification of AE signals

afterwards, and eventually the crack penetrates the bottom surface of the plate.

Many signals were obtained during each stage of fatigue crack propagation. Figure 6 shows the relationship between the load and the normalized cumulative signals per stage for specimen AT2, where each symbol represents an AE signal received by the sensors. Although many signals took place at or near the peak load over mean load, signals also occurred when the load was near or at its minimum. In the stage 'retardation' after load reduction, most of the AE signals were produced by fretting of the fracture surfaces.

As is usually the case, a large number of signals were recorded during the test. They were generated by crack extension from the notch tip and also by extraneous noise sources, and the number of signals increased significantly during yielding of the specimen as it approached final failure. The

signals were classified based on visual examination of their temporal and spectral features. The general procedure followed in the visual classification of the signals is sketched in Fig. 7. The first visual classification is identified and rejected signals from known and unknown noise sources. The second visual classification was carried out by frequency. The signals from test were found to be of six general types based on their spectral characteristics, labeled Type I - Type VI. In Figs. 8~12, the dot line indicates dominant frequency point at each signal types. Type-I has a dominant peak at approximately 0.5 MHz, straddled by two smaller peaks. Type-II has a dominant peak at approximately 0.3 MHz, and also few smaller peaks before and after the main peak. Type-III has a dominant peak at approximately 0.75 MHz, and a small peak at a higher frequency. Type-IV has dominant peaks at approximately 0.3, 0.5 and 0.75 MHz, and also a peak before 0.3 MHz and after 0.75 MHz. Type-V has a dominant peak at approximately 0.15 MHz. Type-VI has dominant peaks at approximately 0.25 and 0.7 MHz and a small peak at a higher frequency.

Typical classified signals are shown in Figs. 8-12. It should be noted that although the spectra are plotted to about 3 MHz, the AE waveforms are strongly modified by the transducer response at frequencies above 1.5 MHz (see Fig. 2). Moreover, signals at higher frequencies are also affected due to averaging over the aperture of the transducers (about 5 mm). However, the spectral amplitudes of all the recorded signals decay rapidly at frequencies above 1.5 MHz and are not used in the source characterization studies. The percentage of the signal type observed from the each stage of the two specimens is shown in Table 1. It should be noted that the Type-VI signals

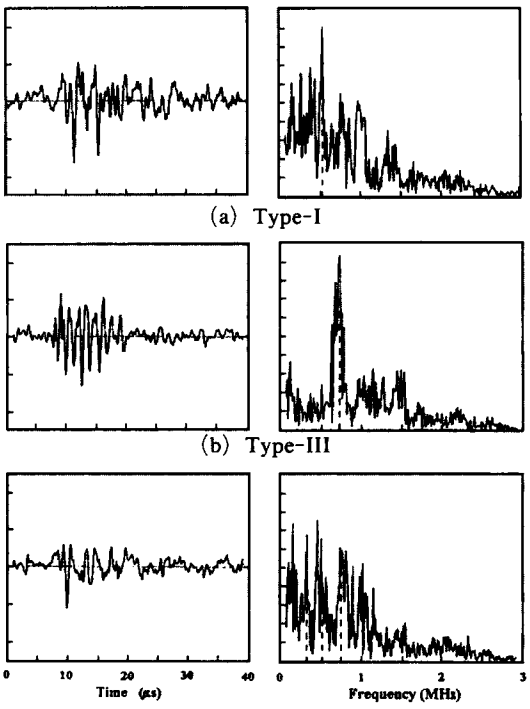

Fig. 8 AE waveforms and their spectra detected at the stage 'pre-penetration' during fatigue crack propagation. Vertical scale is arbitrary

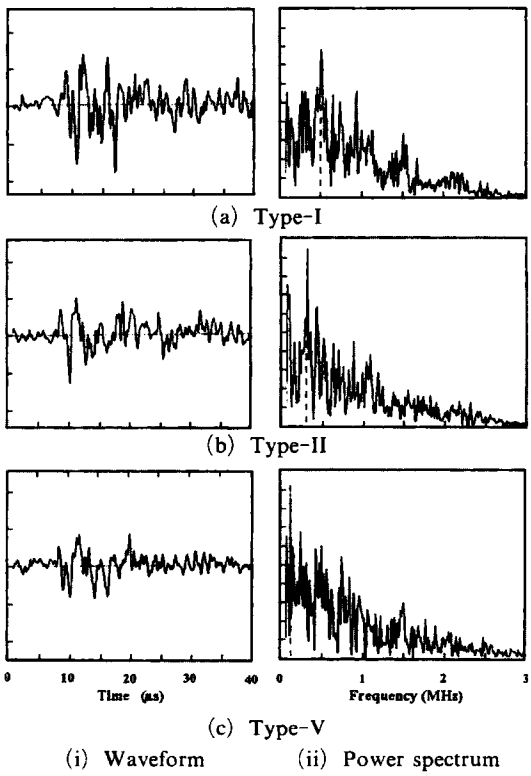

Fig. 9 AE waveforms and their spectra detected in stage 'a' immediately after crack penetration through the back surface of the plate followed by rapid crack growth. Vertical scale is arbitrary

Table 1 Percentage of the signal types obtained from each stage (%)

Specimen	Stages	R	Type-I	Type-II	Type-III	Type-IV	Type-V	Type-VI
AT1	pre-penetration	0.1	42.9	–	6.1	51.0	–	–
	a	0.1	33.3	51.5	–	–	15.2	–
	b	0.1	–	81.5	3.7	–	14.8	–
	c	0.1	90.0	–	–	–	10.0	–
AT2	pre-penetration	0.1	40.7	–	7.4	51.9	–	–
	a	0.1	35.5	54.5	–	–	10	–
	Retardation	0.42	–	4.0	–	–	–	96.0
	b	0.1	–	72.2	–	–	27.8	–
	c	0.1	62.5	–	–	–	37.5	–

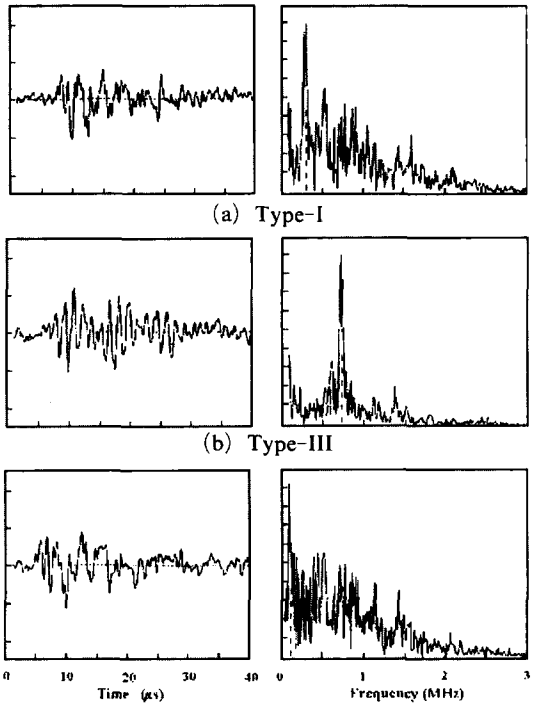

Fig. 10 AE waveforms and their spectra detected in stage 'b' during crack growth at nearly constant rate immediately after penetration. Vertical scale is arbitrary

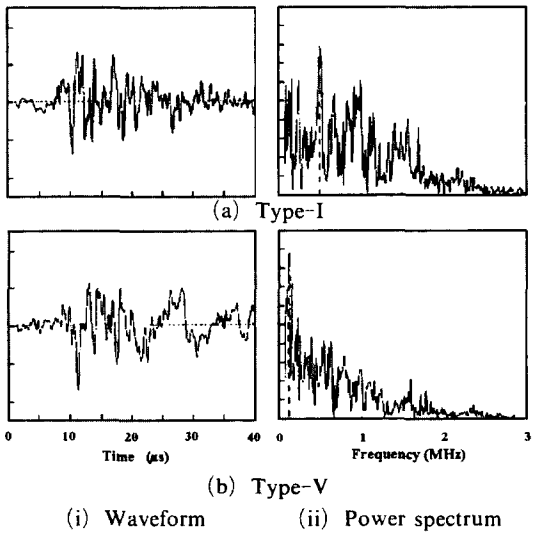

Fig. 11 AE waveforms and their spectra detected in stage 'c' during accelerating crack growth in back surface of the plate. Vertical scale is arbitrary

were obtained from the stage 'retardation' in specimen AT2 only.

The waveforms and power spectra of the signals recorded in stage 'pre-penetration' are shown in Fig. 8. The signals from this stage are of three types : Type-I, Type-III and Type-IV. The signals from stage 'a' are of Type-I, Type-II and Type-V, and are shown in Fig. 9. The signals from stage 'b' can be classified into Type-II, Type-III and Type-V, and are shown in Fig. 10. The signals from Stage 'c', in which the length of the crack trace are about the same on the front and back surfaces of the plate, can be classified into Type-I and Type-V, and are shown in Fig. 11. The waveforms and power spectra of the signals obtained from the retardation stage in specimen AT2, just after penetration, are shown

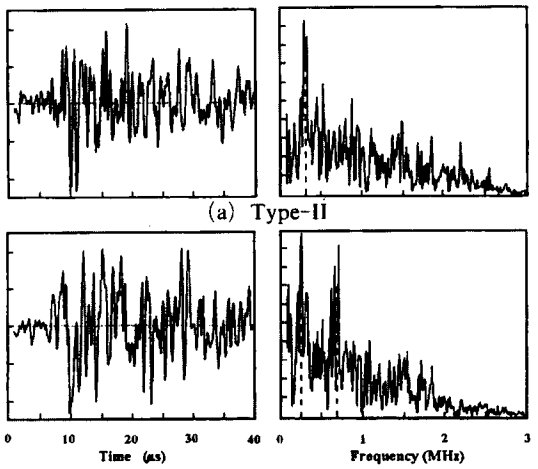

Fig. 12 AE waveforms and their spectra detected during plastic unloading and stage 'retardation' in crack grow. Vertical scale is arbitrary

in Fig. 12. These signals can be divided into Type-II and Type-VI. It can be seen that the main types of signals obtained in each stage for the two specimens are very similar although there are differences in some of their detailed features (see Table 1).

The waveforms of Type I-V signals obtained from the two specimens are characterized by a very sharp rise and decay and very short duration. These are typical characteristics of plate guided extensional and flexural waves (Guo, 1996). The stress ratio was changed from R=0.1 to R=0.42 in order to obtain the signals from fretting in the retardation stage after penetration in specimen AT2. The specimen displayed retardation behavior caused by varying the range of applied stress (Wheeler, 1972). It displayed a large number of signals caused by fretting of the existing fracture surfaces. The waveforms of Type-II and Type-VI obtained from this stage were of significantly longer duration than those observed in the other stages.

In the stage 'pre-penetration', where the crack propagates in three-dimensions, the majority of the signals were of Type-I and Type-IV. Stages 'a' and 'b', after penetration, produced mainly Type-II signals. On the other hand, 96% of the fretting signal in the stage 'retardation' after penetration were of Type-VI. Final fracture, stage 'c', had mainly signals of Type-I, but a little Type-V.

The AE signals detected during the five stages, namely, stage 'pre-penetration', stage 'a', stage 'b', stage 'c' and stage 'retardation', were found to be different. Signals from the stage 'pre-penetration' had a dominant peak at a relatively high frequency (0.5~0.75 MHz), while those from stages 'a' and 'b', after penetration, had dominant peaks at a relatively low frequency of approximately 0.3 MHz. The dominant frequency of the signals from stage 'c' was at about 0.5 MHz. Signals from the stage 'retardation', after penetration, had dominant peaks at approximately 0.25 and 0.7 MHz.

The differences in the properties of the signals can be attributed to the fact that the AE signals are carried by a mixture of high-frequency extensional and lower-frequency flexural plate guided Lamb waves and that the relative amount of the two types of waves depend on the proximity of the crack to the surface of the plate (Wu, 1995; Nam, 2001). As the crack extends through plate thickness, the characteristics of the signals change due to interference between different ratios of the combination of the two types of waves. In addition, different types of AE signals may be generated from crack initiation and propagation as a function of the loading cycle. The AE signals resulting from crack growth near a peak tensile stress can be caused by the fracture of inclusions in the path of the crack (McBride, 1981). Accordingly, it can be concluded that signals obtained from the fatigue tests are generated by crack propagation. As the stress is reduced to zero, the crack may close, and signals may be generated from crack surface fretting. These types of signals have frequency characteristics that are different from those of the signals from crack growth and can be identified as noise. As the stress increases, the crack surfaces that were mechanically adhered can separate and generate AE signals according to crack growth.

5. Concluding Remarks

An advanced waveform-based acoustic emission (AE) technique was applied to study the characteristics of the acoustic emission signals emanating from fatigue crack propagation and penetration in 6061aluminum plates under fatigue loading. The waveforms and power spectra of the signals from the various stages of crack propagation were analyzed by their spectral characteristics. It was found that the AE events increase significantly as the crack approached the back surface of the plate, and decreased just before it penetrated the back surface. Only one type of signal was mainly observed during the stage 'retardation' after crack penetration; this is due to fretting between the crack faces.

From the analysis of the waveforms and their power spectra for a 6061 aluminum plate containing a surface crack, it is possible to monitor, in real-time, the crack propagation and penetration behavior, along with damage and defects in structural members.

References

Ando, K., Fujibayashi, S., Nam, K. W., Takahashi, M. and Ogura, N., 1987, "The Fatigue Life and Crack Through-Thickness Behavior of a Surface-Cracked Plate (for the Case of Tensile Load)," *JSME Int. J.*, Vol. 30, pp. 1898~1905.

Ando, K., Matsushita, H., Fujibayashi, S. and Ogura, N., 1985, "Separation and Fracture Toughness of Controlled Rolled Steel," *J. Society of Materials Science*, Vol. 34, pp. 388~393, (in Japanese).

Choi, C. Y., Kwon, J. D. and Sul, I. C., 2001, "Application of the Leak Before Break (LBB) Concept to a Heat Exchanger in a Nuclear Power Plant," *KSME International Journal*, Vol. 15, pp. 10~20.

Dunegan, H. L. and Harris, D. O., 1969, "Acoustic Emission - A New Nondestructive Testing Tool," *Ultrasonics*, Vol. 7, pp. 160~166.

Elber, W., 1970, "Fatigue Crack Closure under Cyclic Tension," *Engng. Fract. Mech.*, Vol. 2, pp. 37~45.

Fang, D. and Berkovits, A., 1993, "Fatigue Damage Mechanisms on the Basis of Acoustic Emission Measurements," Novel Exper. Techniques in Fracture Mechanics, ed. by A. Shukla, AMD, Vol. 176, *ASME*, pp. 213~235.

Gilchrist, M. D., Chipalo, M. I. and Smith, R. A., 1992, "Shape Development of Surface Defects in Tension Fatigued Finite Thickness Plates," *Int. J. Press. Piping*, Vol. 49, pp. 121~137.

Guo, D., Mal, A. and Ono, K., 1996, "Wave Theory of Acoustic Emission in Composite Laminate," *J. of Acoustic Emission*, Vol. 14, pp. s19~s46.

Huh, N. S., Kwak, D. O., Kim, Y. J., Yu, Y. J. and Pyo, C. R., 2000, "Effect of Nozzle on Leak-Before-Break Analysis Result of Nuclear Piping," *J. KSME. Kor.*, Vol. 24, pp. 2796~2803.

IMCO Resolution A 328(IX), 1975, "Code for the Construction and Equipment of Ships Carrying Liquefied Gases in Bulk".

Kaufman, J. G., Bucci, R. J. and Kelsey, R. A., 1980, "Fracture Mechanics Aspects of the Structural Integrity Technology of Spherical Aluminum Containment Vessels for LNG Tankers," *ASME J. Eng. Mater. & Technology*, Vol. 102, p. 303.

Kawahara, M. and Kurihara, M., 1975, "A Preliminary Study on Surface Crack Growth in a Combined Tensile and Bending Fatigue Process," *Japan Soc. Naval Archit.*, Vol. 137, pp. 297~306, (in Japanese).

Kim, Y. J., Huh, N. S. and Kim, Y. J., 2001, "New Engineering Estimation Method of J-Integral and COD for Circumferential Through-Wall Cracked Pipes," *J. KSME. Kor.*, Vol. 25, pp. 548~553.

Kohn, D. H., Ducheyne, P. and Awerbuch, J., 1992, "Acoustic Emission during Fatigue of Ti-6Al-4V : Incipient Fatigue Crack Detection Limits and Generalized Data Analysis Methodology," *J. of Materials Science*, Vol. 27, pp. 3133~3142.

Liptai, R. G., Harris, D. O., Engle, R. B. and Tatro, C. A., 1971, "Acoustic Emission Techniques in Materials Research," *Int. J. Nondestructive Testing*, Vol. 3, pp. 215~275.

McBride, S. L., Maclachlan. J. W. and Paradis. B. P., 1981, "Acoustic Emission and Inclusion Fracture in 7075 Aluminum Alloy," *J. Nondestructive Evaluation*, Vol. 2, pp. 35~41.

Miyoshi, T. and Yoshida, Y., 1988, "Analysis of Stress Intensity Factor Surface Cracks in Pre and Post Penetration," *Jap. Soc. Mech. Engrs*, Vol. 54, pp. 1771~1777, (in Japanese).

Nam, Kiwoom, 1999, "Acoustic Emission from Surface Fatigue Cracks in SS41 Steel," *Fatigue Fract. Engng. Mater. Struct.*, Vol. 22, No. 12, pp. 1103~1109.

Nam, Ki-Woo and Ahn, Seok-hwan, 2002, "Crack opening behavior of penetrated crack under fatigue load," *KSME International Journal*, Vol. 16, No. 1, pp. 24~31.

Nam, K. W., Ando, K., Ogura, N. and Matui, K., 1994, "Fatigue Life and Penetration Behaviour of a Surface Cracked Plate under Combined Tension and Bending," *Fatigue Fract. Engng. Mater. Struct.*, Vol. 17, pp. 873~882.

Nam, K. W., Ando, K. and Ogura, N., 1993, "The Effect of Specimen Size on the Behaviour of Penetrating Fatigue Cracks," *Fatigue Fract. Engng. Mater. Struct.*, Vol. 16, pp. 767~779.

Nam, K. W., Ando, K. and Ogura, N., 1995, "Surface Fatigue Crack Life and Penetration Behavior of Stress Concentration Specimen," *Engng. Fract. Mech.*, Vol. 51, pp. 161~166.

Nam, K. A. and Ajit, M., 2001, "Characteristics of Elastic Waves Generated by Crack initiation in Aluminum Alloys under Fatigue Loading," *J. Mater. Res.*, Vol. 16, No. 6, pp. 1745~1751.

Sakai, T., Takashima, H., Matsumae, H. and Yajima, H., 1975, "Studies on Nine Percent Nickel Steel for Liquefied Natural Gas Carriers," *ASTM STP*, Vol. 579, pp. 205~237.

Wheeler, O. E., 1972, "Spectrum Loading and Crack Growth," *J. Basic Engng.*, Vol. 90, pp. 181~186.

Wu, J.-U., 1995, "Characterization of Acoustic Emission from Fatigue of 2024-T4 Aluminum using Pattern Recognition," *Mater's Thesis, University of California, Los Angeles*, CA.